Numerical Simulation of Heavy Rainfall in August 2014 over Japan under Pseudo Global Warming Conditions

Y Minamiguchi[1], **H Shimadera**[1], **T Matsuo**[1] **and A Kondo**[1]

1 Graduate School of Engineering, Osaka University, 2-1 Yamadaoka, Suita, Osaka 565-0871, Japan
E-mail: minamiguchi@ea.see.eng.osaka-u.ac.jp

Abstract. This study investigated the impact of global warming on summertime heavy rainfall using the Weather Research and Forecasting model with the pseudo global warming (PGW) method. WRF simulations were conducted for August 2014 over a domain covering Japan, in which two big typhoons attacked Japan and rain fronts frequently passed over, in a baseline and two PGW (RCP4.5 and RCP8.5) conditions. The analysis showed that the future climate led to a larger amount of precipitation than the past climate during the study period in Japan. The mean increase rate of upward moisture supply from the surface of the entire modelling domain was 2.8% K^{-1} in RCP4.5 condition and 3.3% K^{-1} RCP8.5 condition. The mean increase rate of 2-m specific humidity was 6.7% K^{-1} in both RCP4.5 and RCP8.5 conditions, which is comparable to the Clausius-Clapeyron relationship. Therefore, the water supply from the lateral boundaries contributed to the increase in humidity largely and precipitation subsequently. The increases in precipitation related to typhoons were larger than rain fronts, in particular, the changes were remarkable over the paths of typhoons. These results show global warming will significantly increase the summertime heavy precipitation over Japan in the future.

1. Introduction

In recent decades, climate change is proceeding as a consequence of global warming. According to the Intergovernmental Panel on Climate Change (IPCC) Fifth Assessment Report, the climate change causes severe precipitation events with more intense and more frequent rainfall [1]. This is because the saturation pressure of water vapour increases due to the air temperature rise under the global warming, and the water vapour supplied from the sea increases due to the rise in sea surface temperature. Based on the Clausius-Clapeyron (CC) relationship, the atmosphere can hold more moisture in warmer air temperatures with a rate of about 6–7% K^{-1}, and extreme precipitation intensities can also increase by this rate because of global warming [2–5]. While daily extreme precipitation intensities typically increase with a warming atmosphere by within the rate expected from the CC relationship [6,7], changes in shorter duration precipitation extremes may well exceed the rate [6].

The Pseudo Global Warming (PGW) method, which is a dynamical downscaling method proposed by Kimura and Kitoh [8], allows the projections of regional climate change of a specific precipitation event. Several previous studies have applied the method to analyses on Baiu rain front [9] and typhoons [10–12], and reported that global warming should have a large impact on precipitation. In this study, we focused on recent heavy precipitation events observed in August 2014, in which Typhoons Nakri and Halong attacked Japan and rain fronts frequently passed over [13]. The total precipitation of the month was the largest on record for August in western Japan. During this period, torrential rain and storms caused serious damage in Japan such as landslides, inundations, floods, and other disasters. Typhoon Nakri occurred in the east of the Philippines on July 29, 2014, and approached the Okinawa and Amami

Islands from July 31 to August 1. The typhoon caused heavy rain in Japan even after it turned into a tropical depression in the Yellow Sea on August 3. Typhoon Halong, which occurred on the east of Guam on July 29, approached the Daito Islands on August 7. It approached and passed through the Shikoku and Kinki regions in western Japan from August 9 to 10, causing the highest peak precipitation in the series of events. In the last half of the month, rain fronts stagnated near Japan and led to frequent occurrence of intense rainfall events. On August 20, landslides occurred at Hiroshima city following an intense rain of more than 100 mm h^{-1}. During these events, warm and humid air was continuously supplied from south of Japan. In order to evaluate the impact of global warming on record-high summertime precipitation over Japan, this study conducted numerical simulations of the precipitation events in August 2014 using the Weather Research and Forecasting (WRF) model [14] version 3.7 with the PGW method.

2. Methods

2.1. Model configurations

This study focused on the series of heavy rainfall events in August 2014. Figure 1 shows the WRF modelling domain on the Lambert conformal conic projection map, which has an area of 2250 km × 2250 km and covers almost all of Japan. The horizontal resolution and the number of grid cells are 5km and 450 × 450, respectively. The vertical layers consisted of 40 sigma-pressure coordinated layers from the surface to 100 hPa. Figure 1a also shows average sea surface temperature in the study period, which tended to be higher than that in August of 1981–2010 according to the Japan Meteorological Agency (JMA) [15]. As shown in Figure 1b, there are 147 meteorological observatories for validation of WRF simulation in the domain. The area of Japan was divided into eight regions consisting of Hokkaido, Tohoku, Kanto, Chubu, Kinki, Chugoku, Shikoku, and Kyushu. The numbers of observatories in these regions are 18, 17, 17, 30, 11, 14, 9, and 31, respectively.

Static geographical data, objective analysis data, and physical parameterizations used in this study were similar to those used by Shimadera et al. [16]. Topography and land use were derived from the 30-s resolution data of the United States Geological Survey and the 100-m resolution National Land Numerical Information data of the Geospatial Information Authority of Japan, respectively. Initial and boundary conditions in the atmosphere were derived from the mesoscale model grid point value (MSM GPV) data by JMA [17]. Daily sea surface temperature was derived from the high-resolution, real-time, global sea surface temperature analysis data (RTG_SST_HR) by the U.S. National Centres for Environmental Prediction (NCEP) [18]. Initial conditions of variables on the ground surface and in soil layers were derived from the final operational global analysis (FNL) data by NCEP [19]. The MSM GPV data have spatial resolutions of 0.0625° (longitude) × 0.05° (latitude) for ground level data and 0.125° (longitude) × 0.1° (latitude) for pressure level data and a temporal resolution of 3 hours. The RTG_SST_HR data have a spatial resolution of 0.0833° and a temporal resolution of 24 hours. The FNL data have a spatial resolution of 1° and a temporal resolution of 6 hours. The physical parameterizations used in this study include the Yonsei University scheme [20] for the planetary boundary layer parameterization, the WRF single-moment 6-class microphysics scheme [21], the Noah land surface model [22], the rapid radiative transfer model [23] for long wave radiation, and the Dudhia scheme [24] for the shortwave radiation.

Meteorological fields in August 2014 were produced by repeating 5-day simulations with 4-day (from 1st to 4th day) spin-up 31 times. During the spin-up period, the grid nudging for horizontal wind components was applied with a nudging coefficient of 1.0×10^{-4} s^{-1} in the entire simulation domain with the MSM GPV data.

2.2. Experimental design

In order to estimate the sensitivity of precipitation to global warming in the heavy rainfall in August 2014, WRF simulations were conducted in one baseline condition and two PGW conditions (RCP4.5 and RCP8.5). The baseline simulation should reproduce meteorological fields accurately with initial and boundary conditions prepared from MSM GPV, NCEP FNL and RTG_SST_HR datasets. The PGW conditions were prepared with the global bias-corrected climate model output data from the Community

Earth System Model version 1 by the U.S. National Centre for Atmospheric Research [25]. We used datasets for a 20th century simulation (20THC) and two concomitant Representative Concentration Pathway (RCP) future scenarios (RCP45 and RCP85), which are based on the IPCC AR5.

In order to develop PGW fields, averaged climate conditions were calculated from 30-year data for two months (July and August) during 1971–2000 in 20THC for the past and during 2071–2100 in RCP4.5 and RCP8.5 for the future. Then, anomalies of global warming were calculated as the difference between the averaged future and past climate conditions, and were added to the regional climate dataset of the baseline condition. Thus, sets of the PGW conditions were constructed for various meteorological factors, for example, air temperature, humidity, sea surface temperature, sea level pressure and wind speed. Figure 2 illustrates spatial distributions of surface air temperature and sea surface temperature differences in the future conditions (RCP45 and RCP85) from the past condition (20THC). The mean increase amounts over the entire domain of surface air temperature and sea surface temperature from 20THC were 1.4 K and 1.3 K in RCP45 condition, and 3.2 K and 2.7 K in RCP85 condition, respectively. The increase in air temperature was larger than in sea surface temperature, and in regard to spatial distributions, the change in high latitude was larger than in low latitude.

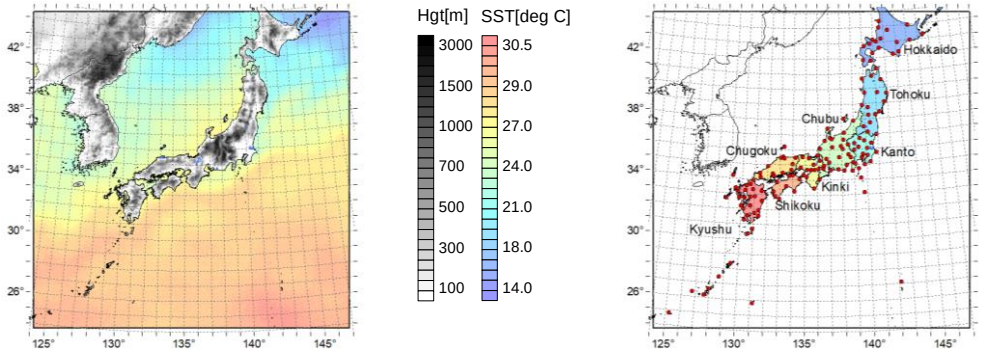

Figure 1. Modelling domains showing (a) topography of land areas and average sea surface temperature of August 2014; (b) locations of meteorological observatories and division of regions for analyses of precipitation.

3. Results and Discussion

3.1. Model Performance

The result of the WRF simulation in the baseline condition was compared with observation data. The index of agreement for all the meteorological observatories was 0.96 for air temperature, 0.95 for specific humidity, 0.85 for wind speed and 0.74 for precipitation. The values indicate high correlations and small biases between the observed and simulated meteorological variables. Figure 3 shows comparisons between observed and simulated monthly precipitations at all the observatories in August 2014. Although the model tended to underestimate at the observatories where the monthly values over approximately 500 mm were observed, most of the simulated values (85%) were within a factor 2 of the observed values. Figure 4 shows spatial distributions of the observed and simulated monthly precipitations in August 2014. The observed precipitation was obtained from the Radar/Raingauge-Analyzed Precipitation data by JMA [26]. The Radar/Raingauge-Analyzed Precipitation data have a spatial resolution of 1 km and a temporal resolution of 30 minutes, and cover areas within a few hundred kilometers from the coastal lines of Japan. Although the simulation slightly underestimated the largest amount of monthly precipitation in the Shikoku region caused by Typhoons Nakri and Halong, it approximately reproduced the spatial variation pattern over the land area in Japan.

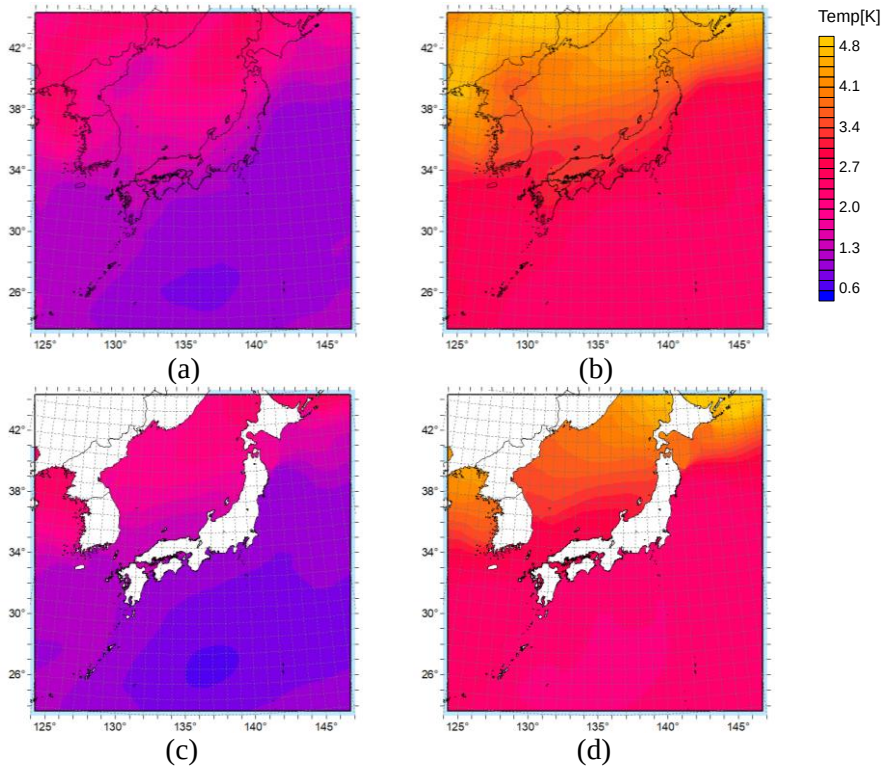

Figure 2. Spatial distributions of surface air temperature differences of the 30-year means for July and August from the past period, 1971-2000, in (a) RCP4.5 and (b) RCP8.5 (2071-2100), and of sea surface temperature differences of the 30-year means for July and August fro m the past period in (c) RCP4.5 and (d) RCP8.5.

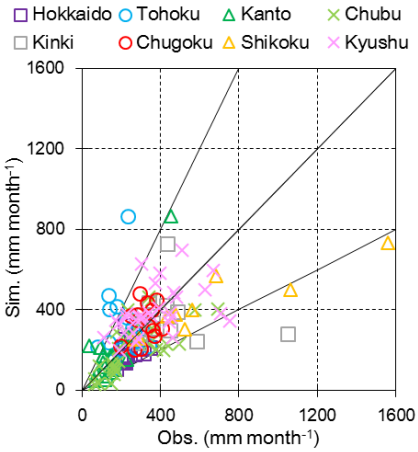

Figure 3. Scatter plots of monthly precipitation at the meteorological observatories in August 2014 for the observation and the simulation results in the baseline condition. The plots are classified as each region.

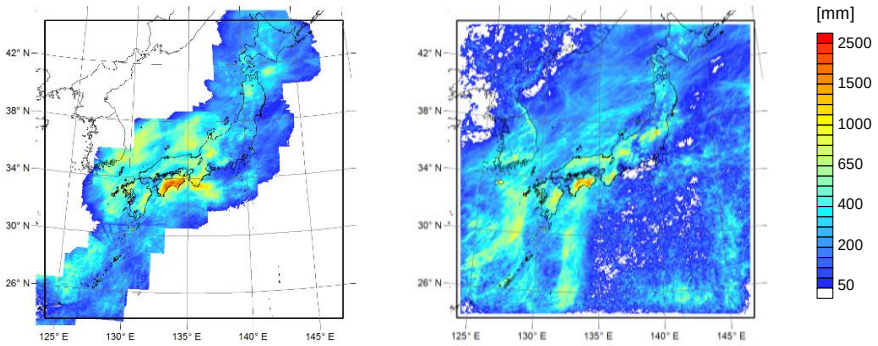

(a) (b)

Figure 4. Spatial distributions of monthly precipitation in August 2014 obtained from (a) Radar/Raingauge-Analyzed Precipitation data and (b) baseline condition. The Radar/Raingauge-Analyzed Precipitation data covers areas within a few hundred kilometers from the coastal lines of Japan.

3.2. Sensitivity under PGW conditions

The sensitivity of precipitation to global warming was analysed in terms of temporal and spatial variations. Figure 5 shows a time series comparison of daily precipitations averaged for all the meteorological observatories in the baseline and PGW conditions. Figure 6 shows monthly precipitation averaged for the meteorological observatories over the land of Japan and each of the eight regions (Figure 1b) in August 2014. Figure 7 illustrates spatial distributions of daily precipitation difference from the baseline condition in the PGW conditions for the first and last halves of the simulation period. Table 1 shows 2-m air temperature, 2-m specific humidity, monthly precipitation and upward water vapour flux averaged over the land area of Japan, the sea area, and the entire area in the modelling domain. The increase in precipitation under PGW conditions, especially under RCP8.5 condition, were remarkable over southern to western Japan including the Kinki and Shikoku regions where there was a large amount of precipitation associated with Typhoons Nakri and Halong during the first half of August 2014. By contrast, there were smaller changes in the amount of precipitation related to rain fronts during the last half of the month. As a result, the mean increase amounts of precipitation under RCP8.5 condition were 4.0 ± 1.7 and 2.2 ± 1.4 mm d^{-1} K^{-1} over the land area of Japan in the first and last halves, respectively. The large difference between the two periods was probably due to the difference in the total precipitation (larger in the first half and smaller in the last), because the difference in the corresponding increase rates (8.6 and 7.5% K^{-1} for the first and last halves, respectively) was less clear.

The mean increase rates of upward moisture supply from the surface of the entire area of the modelling domain to 2-m air temperature increase were 2.8% K^{-1} and 3.3% K^{-1} in RCP4.5 and RCP8.5 conditions, respectively, and the rates of 2-m specific humidity change were larger with the values being 6.7% K^{-1} in both PGW conditions. Based on the CC relationship, as mentioned above, the atmosphere can hold more moisture in warmer air temperatures with a rate of about 6–7% K^{-1}, namely the 2-m humidity increase rates were comparable to the rate of the CC relationship. These results suggested that the most of the increased amount of water were transported from the lateral boundaries, particularly the south one with warm and humid air inflows. The rates of the precipitation change were still larger than the change of the water flux and of the humidity, furthermore localized or in short durations, the rates were much larger than the CC relationship. Additionally, the increasing rate of precipitation to 2-m air temperature in RCP4.5 was larger than in RCP8.5. This is because the saturation pressure of water vapour increases exponentially with air temperature, which resulted in a larger amount of precipitable water under higher temperature condition. It suppressed the increase in precipitation in this research, and it should also enhance the potential for extreme precipitation.

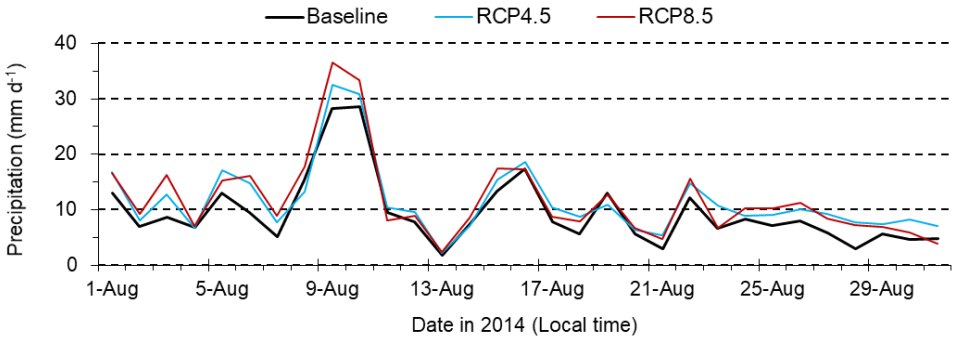

Figure 5. Temporal variations of daily precipitation averaged for all the meteorological observatories in August 2014 for the comparison of the baseline, RCP4.5, and RCP8.5 conditions.

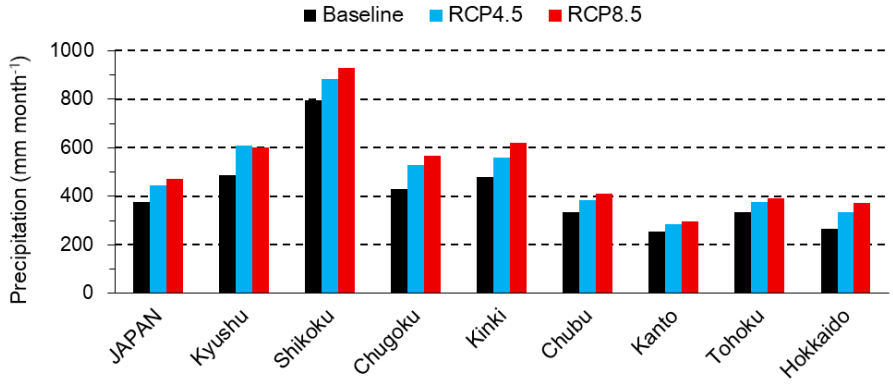

Figure 6. Monthly precipitation averaged over the land area of Japan and each region in August 2014 for the comparison of the baseline, RCP4.5, and RCP8.5 conditions.

4. Conclusions

This study was conducted to investigate the impact of global warming on simulated precipitation fields in the period. Numerical experiments under pseudo global warming conditions were conducted for examining the sensitivity of simulated heavy precipitation to global warming.

Precipitation generally increased under pseudo global warming conditions. The analysis showed that the future climate led to a larger amount of precipitation than the past climate during the study period in Japan. The mean increase rate of upward moisture supply from the surface of the entire area of the modelling domain was 2.8% K^{-1} in RCP4.5 condition and 3.3% K^{-1} in RCP8.5 condition. The mean increase rate of 2-m specific humidity was 6.7% K^{-1} over the entire domain in both RCP4.5 and RCP8.5 conditions, which is comparable to the Clausius-Clapeyron relationship. Therefore, the water supply from the boundary contributed largely to the increase in humidity, and subsequent precipitation. The increases in precipitation related to typhoons were larger than rain fronts, in particular, the changes were remarkable over the paths of typhoons. These results show global warming will significantly increase the summer-time heavy precipitation over Japan in the future.

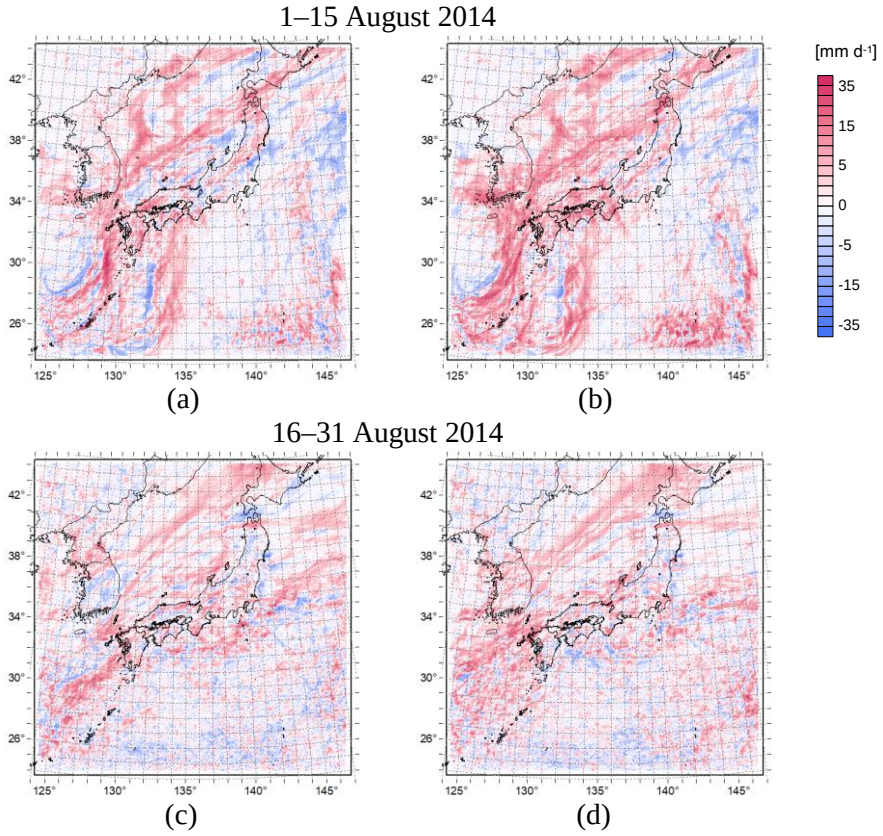

Figure 7. Mean daily precipitation difference from the baseline condition in (a) RCP4.5 and (b) RCP8.5 conditions during the first half of August 2014, and (c) RCP4.5 and (d) RCP8.5 conditions during the last half of August 2014.

Table 1. 2-m air temperature, 2-m specific humidity, monthly precipitation and upward surface water vapour flux averaged over land area of Japan, sea area, and entire area in the modelling domain in the baseline, RCP4.5, and RCP8.5 conditions.

Area	Baseline	RCP4.5	RCP8.5
2-m air temperature (°C)			
Japan	22.2	23.6	25.3
Sea	25.7	27.1	28.6
Domain	24.9	26.3	27.9
2-m specific humidity (g kg^{-1})			
Japan	15.1	16.6	18.4
Sea	18.1	19.6	21.6
Domain	17.2	18.7	20.6
Precipitation (mm month^{-1})			
Japan	376	444	471
Sea	214	251	277
Domain	217	255	279
Upward surface water vapour flux (mm month^{-1})			
Japan	90	91	96
Sea	109	113	120
Domain	107	111	118

5. References

[1] Intergovernmental Panel on Climate Change 2014 *CLIMATE CHANGE 2013: The Physical Science Basis* (Geneva: Intergovernmental Panel on Climate Change) p 7

[2] Boer G J 1993 *Clim. Dyn.* **8** 225–239

[3] Allen M R and Ingram W J 2002 *Nature* **419** 224–232

[4] Trenberth K E, Dai A, Rasmussen R M and Parsons D B 2003 *Bull. Am. Meteorol. Soc.* **84** 1205–17

[5] Pall P, Allen M R and Stone D A 2007 *Clim. Dyn.* **28** 351–63

[6] Lenderink G and van Meijgaard E 2008 *Geosci.* **1** 511–4

[7] Nayak S and Dairaku K 2016 *Hydrol. Res. Lett.* **10** 139–44

[8] Kimura F and Kitoh A 2007 *Final Rep.* (Kyoto: Research Institute for Humanity and Nature) pp 43−6

[9] Kawase H, Yoshikane T, Hara M, Kimura F, Yasunari T, Ailikun B, Ueda H and Inoue T 2009 *J. Geo. Res.* **114** D24110

[10] Ito R, Takemi T and Arakawa O 2016 *SOLA* **12** 100−5

[11] Takemi T, Ito R and Arakawa O 2016 *Hydrol. Res. Lett.* **10** 88−94

[12] Kanada S, Takemi T, Kato M, Yamasaki S, Fudeyasu H, Tsuboki K, Arakawa O and Takayabu I 2017 *J. Clim.* **30** 6017−36

[13] Japan Meteorological Agency 2014 *Prompt report on heavy precipitation in August 2014* (Tokyo: Japan Meteorological Agency) p 1 (in Japanese)

[14] Skamarock W C, Klemp J B, Dudhia J, Gill D O, Baker D M, Duda M G, Huang X –Y, Wang W and Powers J G 2008 *A description of the advanced research WRF version 3; Technical Note TN-475+STR* (Boulder: National Center for Atmospheric Research)

[15] Japan Meteorological Agency http://www.data.jma.go.jp/kaiyou/shindan/index.html (accessed on 8 August 2018)

[16] Shimadera H, Kondo A, Shrestha K L, Kitaoka K and Inoue Y 2015 *Adv. Meteorol.* **2015** 379361

[17] Japan Meteorological Business Support Center http://www.jmbsc.or.jp/jp/online/file/f-online10200.html (accessed on 8 August 2018)

[18] Gemmill W, Katz B and Li X 2007 Daily real-time, global sea surface temperature high-resolution analysis: RTG_SST_HR, NOAA/NWS/NCEP/MMAB Office Note http://polar.ncep.noaa.gov/sst/ (accessed on 8 August 2018)

[19] National Centers for Environmental Prediction/National Weather Service/NOAA/U.S. Department of Commerce 2000 *NCEP FNL Operational Model Global Tropospheric Analyses, continuing from July 1999* (Boulder: National Center for Atmospheric Research) https://doi.org/10.5065/D6M043C6 (accessed on 8 August 2018)

[20] Hong S -Y, Noh Y and Dudhia J 2006 *Mon. Weather Rev.* **134** 2318–41

[21] Hong S -Y and Lim J -O J 2006 *J. Korean Meteor. Soc.* **42** 129–51

[22] Chen F and Dudhia J 2001 *Mon. Weather Rev.* **129** 569–85

[23] Mlawer E J, Taubman S J, Brown P D and Iacono M J 1997 *J. Geophys. Res.* **102** 16663–82

[24] Dudhia J 1989 *J. Atmos. Sci.* **46** 3077–107

[25] Monaghan A J, Steinhoff D F, Bruyere C L and Yates D 2014 *NCAR CESM Global Bias-Corrected CMIP5 Output to Support WRF/MPAS Research* https://doi.org/10.5065/D6DJ5CN4 (accessed on 8 August 2018)

[26] Japan Meteorological Business Support Center http://www.jmbsc.or.jp/jp/offline/cd0100.html (accessed on 8 August 2018)